Issues on Mechanical Properties of 3D Prints

A Major Qualifying Project

submitted to the faculty of the Worcester Polytechnic Institute

in partial fulfillment of the requirements for

the Degree of Bachelor of Science

Project Advisor:

Zhikun Hou

By:

Sean Cody

Peter Pham

Kyle Tyler

Jianqing Zhu

Date: April 25, 2019

Table of Contents

Abstract

This project studied variation of material properties, particularly the Young's modulus, under different 3D prints orientation using three different approaches. Experimentally, we created a testing apparatus that would hold cantilever beam test specimens. The beams are put under various weighted loads and the deflection was measured to calculate the Young's modulus of the material. For numerical analysis, we remade the model with the printing pattern in Solidworks and used finite element analysis to compare experimental results to the theoretical results. We also researched microstructures for justification of variance in 3D prints due to certain print settings. The results have shown that mechanical properties of 3D prints varies with the manufacturing setting, for example, print orientation has an effect on the Young's modulus of 3D prints under print orientation.

1.Introduction

Additive manufacturing has many benefits compared to conventional manufacturing practices such as less waste and the ability to create designs not possible with conventional manufacturing. While the benefits are very much tangible, the actual implementation of additive manufacturing into industry is far from matured.Conventional manufacturing has a much longer history developing since the Industrial revolution of the 18th century. Comparatively, additive manufacturing is still very young only starting to be developed in the 1980's (Gardan, 2016).

In this project we studied the Young's modulus of 3D prints in an attempt to explain some aspects of the gaps between design expectations and print results, specifically with PLA in Fused Deposition Modeling (FDM). Our attempt to explain the gap is done in three major parts: experimental analysis, numerical analysis, and microstructure justification. The goal of the experiment is to isolate variables and collect data of observed results for analysis. To justify our results we apply numerical analysis through finite element analysis to compare theoretical results to .Then we look towards material science as an additional source for explaining our observed results. This report summarizes the development process of our experiment, development of our 3D model for finite element analysis, microstructure analysis, and a review of all results and analyses.

2. Background

In the manufacturing industry, there is 7.6 billion tons of solid, non-hazardous waste produced annually ("Manufacturing and Industrial: Waste Minimization", 2018). In order to mitigate global issues caused by human waste, the manufacturing sector is a realm that can be greatly improved through additive manufacturing.

Our goal is to conduct a series of experiments to better understand mechanical properties of additive manufactured objects. Through doing this, we can better influence the predictability of these objects, allowing for more reliable implementation in industry.

In this literature review, we will examine additive manufacturing, while focusing on aspects relevant to our project. This literature will cover the market for additive manufacturing as well as the industry outlook, the types of printers commonly used in industrial additive manufacturing, the types of materials commonly used in additive manufacturing, important mechanical material properties and their importance in industry, and current state of numerical analysis and simulations of 3D prints.

2.1 Additive Manufacturing Market

In the past 10 years, the economy has seen an intense surge for 3D printers. Given benefits such as versatility in manufacturing, zero-waste, and decreasing cost of use, 3D printers have solidified their presence in the commercial sector as well as industry. In 2014, the market was valued at $4.16 billion (Sawant, 2018). According to the Wohler Report of 2018, the Additive manufacturing industry, including all worldwide AM products and services was 7.336 billion, a 21% increase from the year before ("Wohlers Report 2018: 3D Printer Industry Tops $7 Billion"). In 2025, the market is projected to reach $44.93 billion (Sawant, 2018).
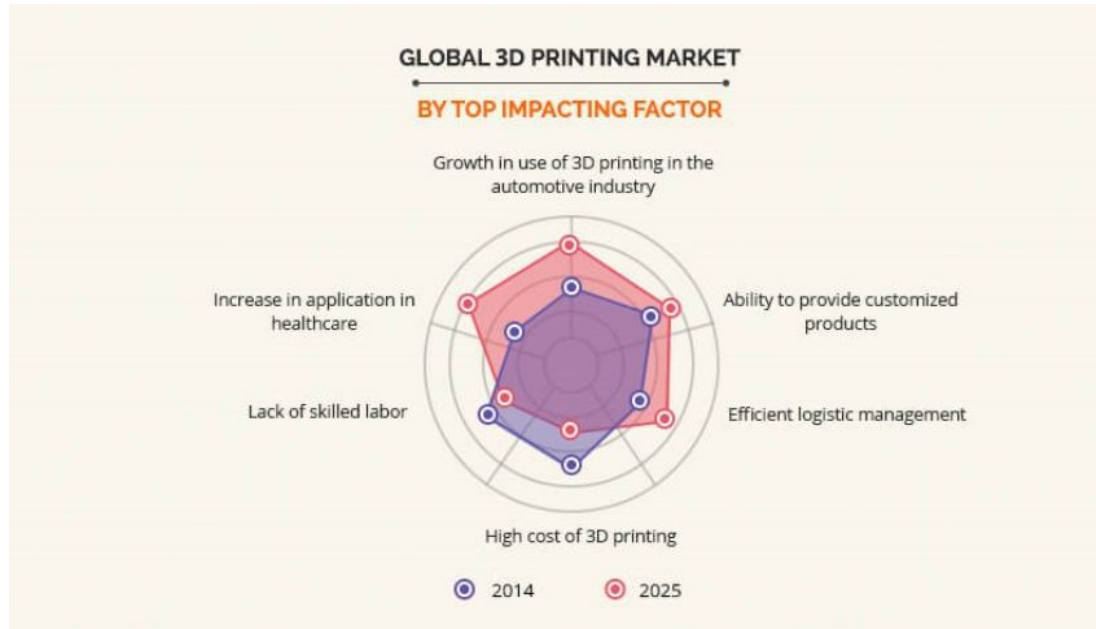
Figure 1. Impacting Factors on AM Market. This figure shows the major playing factors in the additive manufacturing market from 2014 to 2025 (McCue, 2018).

This immense growth is categorized as hardware, software, and services. Hardware currently represents nearly 60% of all the global market share for 3D printing, software represents 30% of the market, and services account for 10% of the market ("3D Printing Market Size", 2017). Hardware includes 3D printers, both desktop size and industrial size. In 2015, it is estimated that more than 278,000 desktop 3D printers under $5,000 were sold worldwide (McCue, 2018). Of these printers, 19% of them were FDM segment printers, holding the largest share of the market in terms of printer type ("3D Printing Market Size", 2017). With the rapid growth of printers, the market for filaments has seen growth similarly. The market for additive manufacturing filaments in 2015 was $204 million and is projected to grow twenty-fold in the next ten years, reaching $4.5 billion in 2025 ("SmarTech Report Show Low-Cost 3D Printing Market Is Alive and Healthy", 2018).
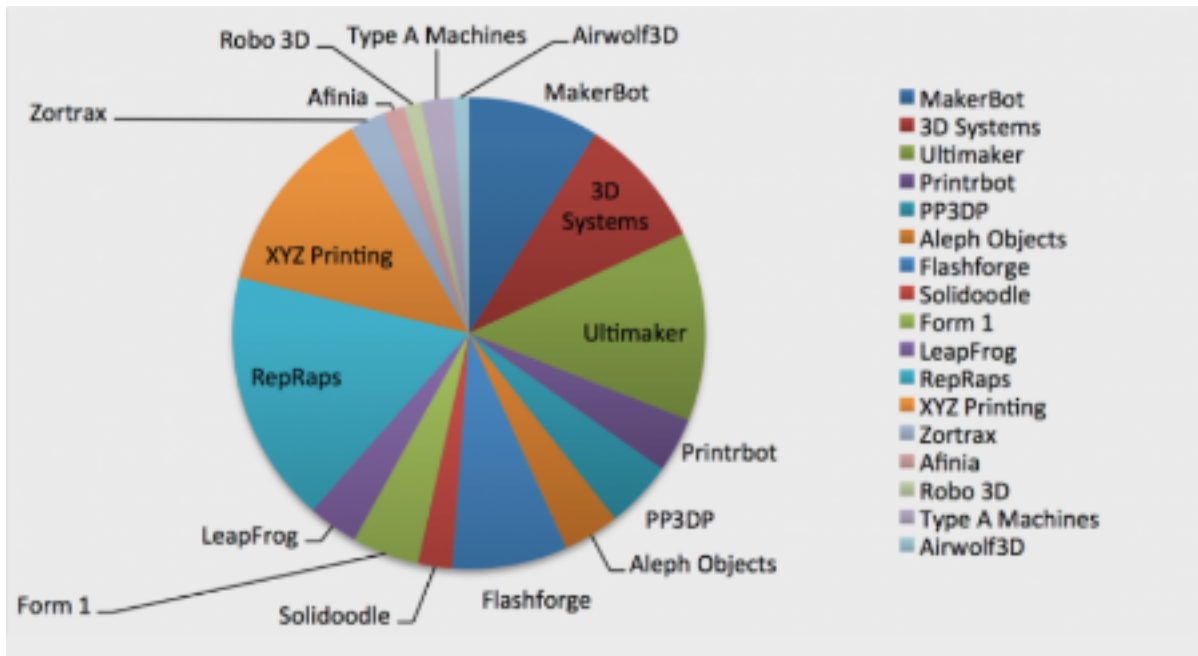
Figure 2. Market Breakdown by Companies. This figure shows the additive manufacturing market share breakdown by companies.

Since additive manufacturing is so fresh to the market, few companies have proven to be leaders in revenue. A SmarTech report analyzing the 2016 3D printing market has shown that market new leaders accounted for 37.6% of the market share in 2015, while historic leaders accounted for only 17.8% ("SmarTech Report Show Low-Cost 3D Printing Market Is Alive and Healthy", 2018). This indicates that the market is extremely new and big companies are competing for their market shares. This competition drives new innovations and lower costs. Popular companies in the additive manufacturing market include RepRaps, Ultimaker, XYZ Printing, Makerbot, and Flashforge ("SmarTech Report Show Low-Cost 3D Printing Market Is Alive and Healthy", 2018).The breakdown of company revenues is shown in figure X. In all, 135 companies in the world are recorded having sold industrial additive manufacturing systems ("SmarTech Report Show Low-Cost 3D Printing Market Is Alive and Healthy", 2018). This doesn't include several fortune 500 companies that have diversified their own manufacturing sectors to include additive manufacturing. These companies include Airbus, Adidas, Ford, Toyota, and General Electric ("SmarTech Report Show Low-Cost 3D Printing Market Is Alive and Healthy", 2018). Currently, North America is leading in the number of 3D printed parts, holding 49.4% of the market ("3D Printing Trends 2019", 2019). With new companies launching every year, large companies diversifying to

include additive manufacturing, and such a significant presence already in North America, it is easy to see why extensive research on additive manufacturing is something that should be supported in academia and industry.
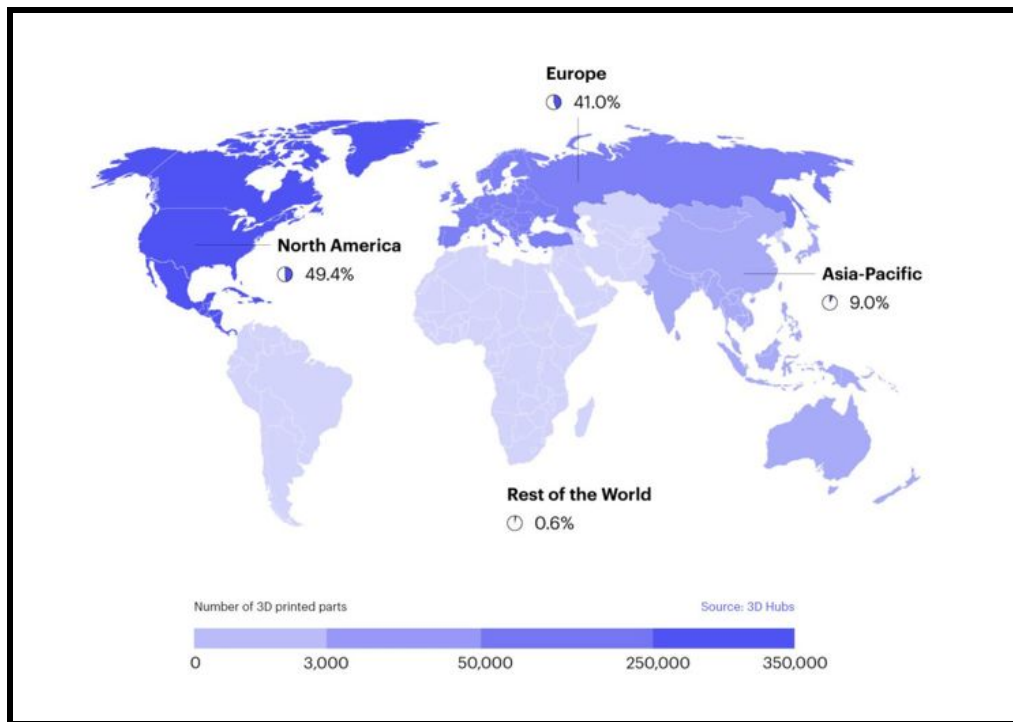
Figure 3. Total Units of Additive Manufacturing by Region. This figure shows the breakdown of total additive manufacturing usage by region of the world.

2.2 Types of Printers

2.2.1 Stereolithography (SLA)

SLA is a fast form of prototyping. The applications for this type of printer involves immense precision and accuracy. SLA produce objects from 3D CAD data (computer-generated files) in just a few hours. This is a 3D printing process that's popular for its fine details and exactness. Machines that use this technology produce unique models, patterns, prototypes, and various production parts. They do this by converting liquid photopolymers (a special type of plastic) into solid 3D objects, one layer at a time. The plastic is first heated to turn it into a semi-liquid form, and then it hardens on contact. The printer constructs each of these layers using an ultraviolet laser, directed by X and Y scanning mirrors. Just before each print cycle, a recoated blade moves across the surface to ensure each thin layer of resin spreads evenly

across the object. The print cycle continues in this way, building 3D objects from the bottom up. (3D Hubs Knowledge Base)
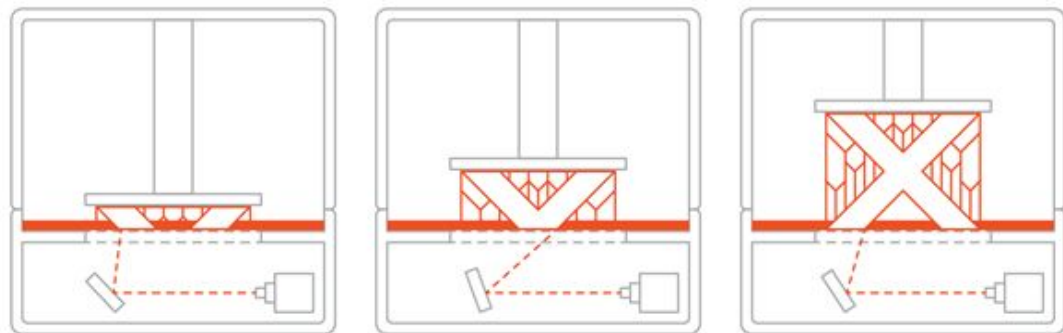

Figure 4: SLA demonstration (from https://www.3dhubs.com/knowledge-base/)

2.2.2 Digital Light Processing (DLA)

DLP is the oldest of the 3D printing technologies, created by a man name Larry Hornbeck in 1987.(http://www.ti.com/dlp-chip/overview.html) It's similar to SLA, given that it also works with photopolymers. The liquid plastic resin used by the printer goes into a translucent resin container. There is, however, one major difference between the two, which is the source of light. While SLA uses ultraviolet light, DLP uses a more traditional light source, usually arc lamps. This process results in impressive printing speeds. When there's plenty of light, the resin is quick to harden in a matter of seconds. Compared to SLA 3D printing, DLP achieves quicker print times for most parts. The reason it is faster is because it exposes entire layers at once. With SLA printing, a laser must draw out each of these layers, and this takes time.

2.2.3 Fused Deposition Modeling (FDM)

FDM is a 3D printing process developed by Scott Crump, and then implemented by Stratasys Ltd. in the 1980s.(https://www.stratasys.com/corporate/about-us) It uses production grade thermoplastic materials to print its 3D objects. It's popular for producing functional prototypes, concept models, and manufacturing aids. It's a technology that can create accurate details and boasts an exceptional strength to weight ratio.

Before the FDM printing process begins, the user has to slice the 3D CAD data (the 3D model) into multiple layers using special software. The sliced CAD data goes to

the printer which then builds the object one layer at a time on the build platform. It does this simply by heating and then extruding the thermoplastic filament through the nozzle and onto the base. The printer can also extrude various support materials as well as the thermoplastic. For example, to support upper layers, the printer can add special support material underneath, which then dissolves after the printing process. As with all 3D printers, the time it takes to print all depends on the objects size and its complexity.
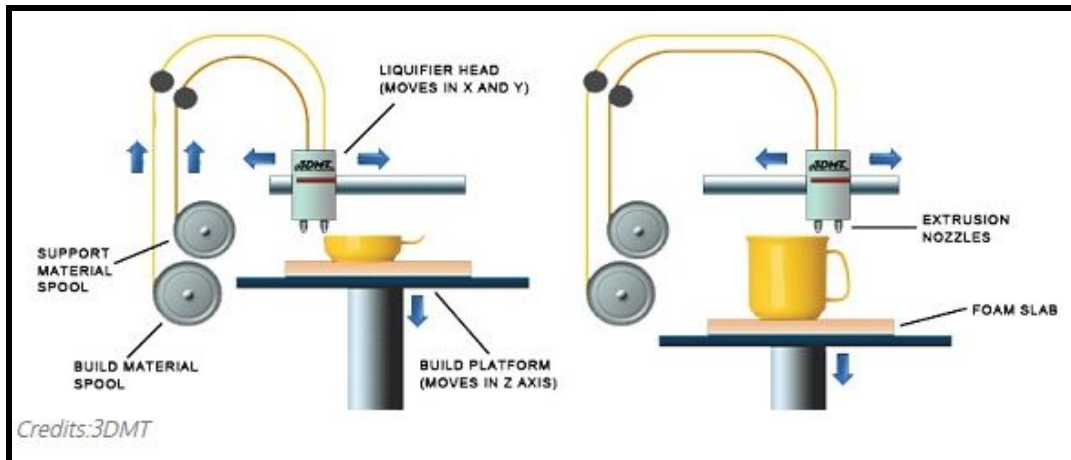
Figure 5: FDM Demonstration (from All3DP)

2.2.4 Selective Laser Sintering (SLS)

An American businessman, inventor, and teacher named Dr. Carl Deckard developed and patented SLS technology in the mid-1980s.(Selective Laser Sintering, Birth of an Industry Dec 6th, 2012) It's a 3D printing technique that uses high power CO2 lasers to fuse particles together. The laser sinters powdered metal materials (though it can utilize other materials too, like white nylon powder, ceramics and even glass). The build platform, or bed, lowers incrementally with each successive laser scan. It's a process that repeats one layer at a time until it reaches the object's height. There is un-sintered support from other powders during the build process that surround and protect the model. This means the 3D objects don't need other support structures during the build. Someone will remove the un-sintered powders manually after printing. SLS produces durable, high precision parts, and it can use a wide range of materials. It's a perfect technology for fully-functional, end-use parts and prototypes. SLS is quite similar to SLA technology with regards to speed and quality. The main difference is with the materials, as SLS uses powdered substances, whereas SLA uses liquid resins. It's

this wide variety of available materials that makes SLA technology so popular for printing customized objects.

2.2.5 Selective Laser Melting (SLM)

SLM made its debut appearance in 1995. It was part of a German research project at the Fraunhofer Institute ILT.(patent DE 19649865) Like SLA, SLM also uses a high-powered laser beam to form 3D parts. During the printing process, the laser beam melts and fuses various metallic powders together. As the laser beam hits a thin layer of the material, it selectively joins or welds the particles together. After one complete print cycle, the printer adds a new layer of powered material to the previous one. The object then lowers by the precise amount of the thickness of a single layer. When the print process is complete, someone will manually remove the unused powder from the object. The main difference between SLM and SLS is that SLM completely melts the powder, whereas SLS only partly melts it. In general, SLM end products tend to be stronger as they have fewer or no voids.

2.2.6 Electron Beam Melting (EBM)

A Swedish company called Arcam AB founded EBM® in 1997.(EBM® Electron Beam Melting n.d.) This is a 3D printing technology similar to SLM , in that it uses a powder bed fusion technique. The difference between the two is the power source. The SLM approach above uses high-powered laser in a chamber of noble, or inert gas. EBM, on the other hand, uses a powerful electron beam in a vacuum. Aside from the power source, the remaining processes between the two are quite similar. The major us of EMB is to 3D print metal parts. Its main characteristics are its ability to achieve complex geometries with freedom of design. EBM also produces parts that are incredibly strong and dense in their makeup.

2.2.7 Laminated Object Manufacturing (LOM)

A Californian company called Helisys Inc. (now Cubic Technologies), first developed LOM as an effective and affordable method of 3D printing. A US design engineer names Michael Feygin, a pioneer in 3D printed technologies, originally patented LOM. LOM is a rapid prototyping system that works by fusing or laminating layers of plastic or paper using both heat and pressure. A computer-controlled blade or

laser cuts the object to the desired shape. Once each printed layer is complete, the platform moves down by about 1/16th of an inch, ready for the next layer. The printer then pulls a new sheet of material across the substrate where it's adhered by a heated roller. This basic process continues over and over until the 3D part is complete.

2.2.8 Binder Jetting (BJ)

BJ is a 3D printing process that uses two types of materials to build objects: a powder-based material and a bonding agent. As the name suggests, the "bonding" agent acts as a strong adhesive to attach (bond) the powder layers together. The printer nozzles extrude the binder in liquid form similar to a regular 2D inkjet printer. After completing each layer, the build plate lowers slightly to allow for the next one. This process repeats until the object reaches its required height.

2.2.9 Material Jetting (MJ)

Unlike other 3D printing technologies, there isn't a single inventor for material jetting.(Introduction to material jetting) In fact, up until recent times it's been more of a technique than an actual printing process. It's something jewelers have used for centuries. Wax casting has been a traditional process where the user produces high-quality, customizable jewelry. The reason it is mention here is because of the introduction of 3D printing. Thanks to the arrival of this technology, wax casting is now an automated process. Today, MJ 3D printers produce high-resolution parts, mainly for the dental and Jewelry industries,

For jewelers who want to experiment with various casts, MJ is now their leading 3D technology. At the time of writing, there are a few high-quality professional wax 3D printers on the market. Once the 3D model (CAD file) is uploaded to the printer, the whole system starts to operate. The printer adds molten (heated) wax to the aluminum build platform in controlled layers. It achieves this using nozzle that sweep evenly across the build area. As soon as the heated material lands on the build plate it begins to cool down and solidify (UV light helps to cure the layers). As the 3D part builds up, a gel-like material helps to support the printing process of more complex geometries. Like all support materials in 3D printing, it's easy to remove afterwards, either by hand or by using powerful water jets. Once the part is complete you can use it right away, no further post-curing necessary.

2.3 3D Printing Variables

According to another study, "the mechanical properties of 3D-printed parts vary depending on the following factors: material used (brand, density, molecular weight, quality,etc), Additive Manufacturing technology used, infill percentage, printing orientation (build and raster), layer height (resolution), infill pattern, cross-sectional area, post-processing (method and time), and others (Dizon, Espera, Chen, Advincula, 2018, p.61)." Below each variable is defined:

Material used - Depending on the type of material mechanical properties can vary greatly. Even within the same material categories properties can vary due to a brand's production process, quality of production, and material recipe. Examples of materials provide in section 2.4.

Additive Manufacturing technology used - As described in section 2.2 the variety of processes and technology in additive manufacturing self evidently has an effect on the mechanical properties of 3D printed parts.

Infill - Infill is the repetitive internal structures found in 3D prints. These internal structures saves the amount of material used while still maintaining support. The variables for infill include:

● Infill pattern is the type of structure printed inside 3D prints.
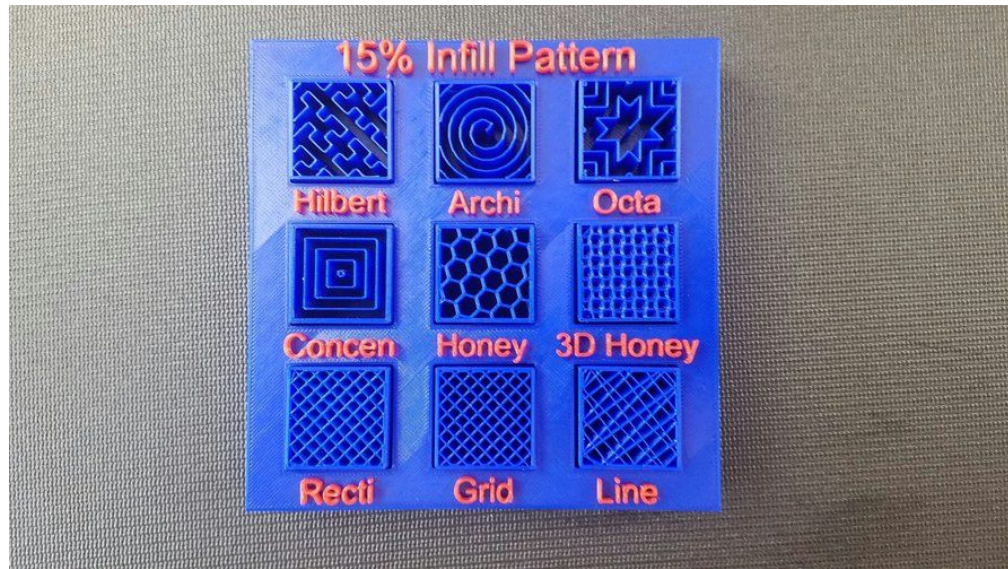

Figure 6: Examples of 3D printing patterns
(Siber, 2018)

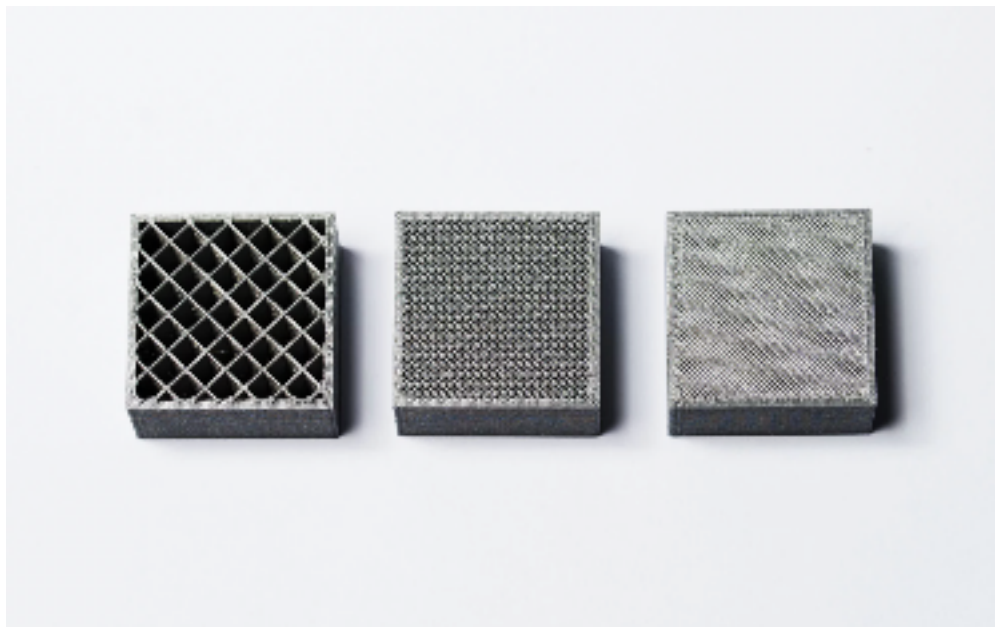● Infill percentage defines the density of the internal structure pattern.

Figure 7: Example of various infill percentages for grid pattern
(Siber, 2018)

Print Orientation - Print orientation is the direction in which the 3D model is laid out in the XY plane to be printed. Orientation of the model is altered by rotating the model in 3D printing software.

Layer height - As given by the name layer height is how high or thick a layer is when printing. The layer height variable determines the speed, resolution, and smoothness of the print ("3D Printing Layer Height", Grames). A smaller layer height has higher resolution and smoothness but requires more time due to placing more layer for the same height. Conversely a larger layer height is faster at the cost of resolution and smoothness.

2.4 Printing Materials

There are many materials used for 3D printing, ranging from plastics, to woods and metals. This project will focus on the plastics used in 3D printing, providing in depth research on Polylactic Acid (PLA), Acrylonitrile Butadiene Styrene (ABS), PolyEthylene Terephthalate (PET), and Nylon.

2.4.1 PLA (Polylactic Acid)

PLA is a thermoplastic that is derived from the fermentation of corn starch in contrast to the petrochemical-derived plastic counterparts (Lunt, 1997). PLA has been popularized by this aspect due to its derivation from a renewable resource and ability to be recycled. In the category of thermoplastics PLA is the most popular material that works with FDM printing, by itself taking up 33% of 3D printing material market shares as of July 2018 (Statista, 2018). The notable properties of PLA are that it is food safe, biodegradable and UV resistant(3D Matter, n.d.). A drawback to PLA is that it has a low humidity resistance. When PLA is left in open air or in a humid environment, the quality of the PLA degrades over time. When printing with humidity degraded PLA the finishes prints are often of poor quality or in some cases unable to print through the extruder of a printer.

2.4.2 ABS (Acrylonitrile Butadiene Styrene)

ABS is another popular thermoplastic produced by polymerizing styrene and acrylonitrile in the presence of polybutadiene ("What is ABS", n.d.). ABS is popular due to its low production costs and ability to be recycled by liquefaction. The notable properties of ABS are that it is impact resistant, chemical resistant, heat resistant and has higher structural strength (3D Matter, n.d.). The drawbacks to ABS are its low UV resistance and potentially toxic fumes when burnt. ABS low UV resistance limits its outdoor usage due to the sun's UV rays. Over time ABS degrades in sunlight by losing its color, cracking, and eventually turning to powder where the cracks develop.

2.4.3 PET (PolyEthylene Terephthalate)

PET is an extremely common material often recognized as the plastic used in water bottles. The notable properties of PET are that it is food safe, waterproof and is chemical resistant. The drawbacks to PET are its wide range of printing temperatures and low humidity resistance prior to printing. PET's wide printing temperature ranges can also be seen as a feature for its printability on almost all printers, however the wide range of temperatures leads to more variation in printing results. Unless the user is experienced with printing in PET, printing temperatures often have to be tweaked. And like PLA its low humidity resistance prior to printing leads to quality degradation.

2.4.4 Nylon

Nylon is a popular material due to its high strength, durability, and flexibility when printed with thin walls. The reason Nylon is not as popular as PLA or ABS is because of its difficulty to be printed properly. Nylon filament requires temperatures above 240 degrees celsius to be printed which is above the operating temperatures of standard extruders. Often printers must be modified with an all metal hot end to handle the high temperatures required for Nylon. Also Nylon is very hygroscopic and must be stored properly in an airtight container like PLA and PET. Prior to printing it is recommended for Nylon to be dried in an oven for 6 to 8 hours to ensure proper printing and to be stored with dessicant to maintain dryness (3D Printing with Nylon).

2.5 Numerical Studies for Analyzing 3D Printed Models

2.5.1 Current Status of Numerical Studies for 3D Printing Applications

Despite the large amount of growth in 3D printing applications, there are a very limited number of programs available to analyze them (Molitch-Hou, 2016). This is due to several factors. For instance, 3D printers are used commonly for prototyping due to their relatively cheap cost and the elimination of any leftover material. Therefore, 3D printed models are primarily used to test the shape of the product, to see if the design would function without having to use a more conventional (and possibly more expensive) material. Due to this, things like stress analysis, thermal analysis, etc. are not considered for 3D printed models, since they are made with material that wouldn't be used for the finished product. Another problem is that 3D filament is more difficult to analyze. When designing a part in a CAD modeling software such as SolidWorks, the material is always considered to be completely solid. With 3D printers, however, you can select the infill, or how close to a solid model you would like the print to be. To save money, 3D prints are usually constructed with a less than 100% infill, meaning you couldn't analyze a 3D printed part as a solid model. As a result of these factors, what does exist for analytical analysis falls under two categories: finite element analysis and simulation programs

2.5.2 Finite Element Analysis (FEA)

Finite element analysis (FEA) is one of the most common numerical analysis program. As such, FEA is a staple of any solid modeling application. Common examples include SolidWorks, Creo, ANSYS, and Calculix, and are present in essentially any CAD software. FEA can compute many kinds of numerical analyses, including thermal, static, and motion. FEA programs work by dividing a potentially complex model into thousands of tiny pieces. Depending on the processing power of the computer or how precise one wishes the calculations to be, FEA can reach into the millions of pieces. Once the model is sufficiently divided, the programs performs calculations of each of the pieces, determining individual stresses, temperatures, etc. Finally, the program reassembles the pieces, resulting in a completed analysis in which one can see the spectrum of results and pinpoint potential areas of interest, such as in the model shown below. A problem that FEA programs run into is that in order to accurately test the model one must know all the forces acting on it. Complex forces such as wind or inconsistent variables such as changes in temperature can make analysis difficult. In addition, each of these forces and variables must be manually

inputted into the FEA program, meaning a complex model or a multi-component assembly becomes increasingly consuming to analyze.
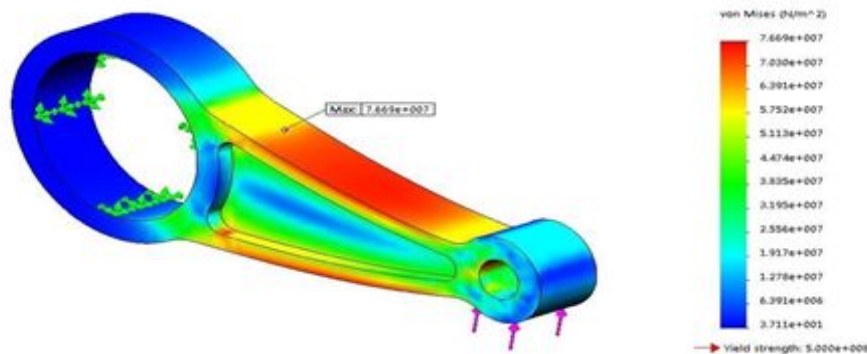

Figure 8: FEA analysis using SolidWorks (from "Finite Element Analysis" n.d.)

2.6.3 Simulation Programs

Simulation programs are essentially hyper-specialized FEA programs, typically created to perform very specific analyses on a very specific type of model. Simulation programs include STAAD, RISA, and SAFE. These programs deal with a much larger analyses than FEA programs, with the benefit of being pre-programmed with the necessary coding to perform them. Simulation programs are often used by civil engineers and architects in the design of buildings, like the design below. Designers can create their model, in this case a building with all its components, and then perform the necessary analyses with ease. This is because the simulation program comes equipped with the necessary calculations that one would have to input manually with a FEA program. Forces like wind, shaking from an earthquake, and the general stress of having people inside the building are already set. All one needs to do is indicate the strength of these forces, and the program will do all the complex calculations for you. Consequently, simulation programs are extremely useful for the specific area of analysis they cover. However, since these programs are highly specialized, they also don't cover many other areas. One would find difficulty modeling a chair with a program designed for a building. As of now, no program exists for 3D printed models, but hopefully one day they will be added or integrated into FEA software.
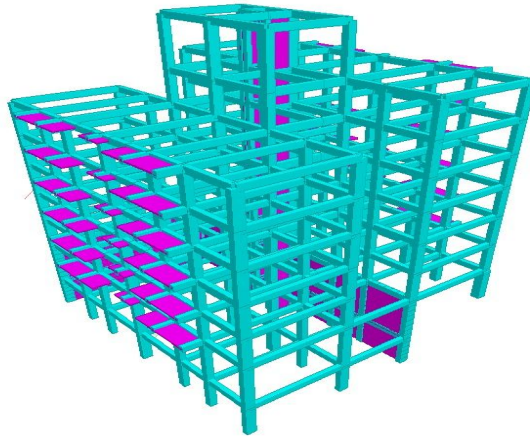
Figure 9: Design of a Building Structure using STAAD Pro (from "STAAD Pro and Spreadsheets", 2011)

3. Experimentation

3.1 Experimentation Methods

Our goal of this project was to identify underlying mechanical characteristics of additive manufacturing print orientation of Polylactic Acid (PLA). As the industry slowly transitions to a more waste-free form of manufacturing, additive manufacturing stands forefront as the most viable alternative to ensure minimal waste. In order for this transition to occur, we must be able to predict mechanical characteristics of the materials used. To achieve our experimentation goals, we had to follow five main objectives: 1. Define an experiment designed to test the mechanical properties of PLA, 2. select experimental components, 3. calibrate system under known values, 4. test PLA specimens, 5. verify findings. The findings can then serve as a guideline to maximize mechanical properties for future use of PLA specimens.

3.1.1 Define Experiment and Components

To complete our first objective, we need to know which mechanical characteristic we wish to test. Through mechanical engineering experience and reviewing relevant literature, we decided to test the Young's Modulus of the PLA. The Young's Modulus is an important mechanical property that measures the stiffness of a solid material in tension and compression. This value defines the stress (force per unit area) in relationship to strain (unit deformation).

Next, we needed to select the medium in which we would measure Young's Modulus. Given research and experimental experiences learned at WPI we decided to perform beam deflection experiments to record deflection of 3D-printed beams. This experiment is beneficial to use because it is easy to accurately obtain measurements and it helps identify key properties of the specimen. The guidelines for the procedure for this experiment will be developed using the following objectives.

Apparatus Selection

For this objective, we had to select an apparatus that would be able to aptly measure beam deflection to allow us to record the Young's Modulus values for beams. This apparatus needed to have accuracy and repeatability. In order to ensure that our specimens were accurately measures, this apparatus needed to have a means of measuring accurately. An accurate measuring system will have a vertical ruler lined up with the end of the specimen to allow for accurate visual recording of quantities. Lastly, this apparatus needed to be secure enough to withstand loads without deformation.

Testing Environment/Set Up

One component of our beam deflection experiment that we needed to ensure was kept constant was the testing environment. With a project consisting of many repetitions and run-throughs, one way to keep the environmental factors constant is to use the same location for each series of testing. This will ensure that external factors that are beyond our control are minimized. Another reason to use the same testing location is that it will help ensure that the same set-up procedure will be followed. By

following the same set-up procedure of clamping the apparatus to the testing table, we will reduce error in our results.

Load Determination

Another component that we had to characterize was our loads that would be applied to our cantilever beam, and how we will attach these loads to our specimens. After researching various Young's Moduli of plastics, we decided on our set of masses to apply. The main consideration in this step was to ensure that the mass was large enough to cause a noticeable deflection on our specimen. That considered, we also had to ensure that the mass applied was not too large, causing mechanical failure of the specimen. Next, we had to determine how we would attach the loads to the end of the specimen so that the load would be distributed evenly throughout the entire end of the specimen. We also had to ensure that the load was applied to the same location on the specimen. This ensured that the deflection was measured over the exact same length every time, thus allowing for more accurate findings. Lastly, we had to determine which type of material we would use that would be strong enough to support the hanging mass. This material had to maximize strength while minimizing weight. Any significant weight would alter the results of our deflection experiment.

Specimen Print Variables

The most important experimental component that we had to determine was the print variables of our specimens. For this, we completed preliminary research on mechanical testing of 3D printed beams. Our goal in this research was to find out specific printing variables that have been vastly researched, so we can shy away from focusing on these variables. We wanted our testing to provide new data to the realm of additive manufacturing. Another factor that lead us to decide the variable we wanted to test was the options provided by the WPI Foisie Labs' 3D Printers.

3.1.2 System Calibration

In order to ensure the accuracy of our apparatus, we needed to calibrate it using a known value. For this we chose to use a metal alloy with a known Young's Modulus.

In order to keep all experimental values constant, we used an alloy of similar dimensions, so the specimen would fit in the apparatus with as much ease as the PLA specimens. We then applied loads ranging from 100g to 500 g to the metal beam and measure the deflection under each load. With the recorded deflections under each load and known dimensions, then applied the values to the moment of inertia formula found in Figure X. and calculated the corresponding Young's Modulus. We completed this experiment on three separate specimens of known alloy. We then compared our experimental values to known values and found a percent error. We decided that any error under 3% would be ideal enough to deem our system accurate.

3.1.3 Testing Requirements

Under this objective, we collected quantitative data for our project that was heavily used to cite in conclusions drawn about the Young's Modulus of 3D-printed PLA. For this objective, we drafted CAD models of our PLA specimen to resemble a beam. We chose a flat, rectangular shape because it was a shape that worked with the printers available and it worked with our experimentation requirements. We then decided to print a series of specimens of PLA with a specific variable manipulated. Following the defined experiment, we completed many experiments to identify mechanical properties within the specimen. We deemed our findings reliable if they had a percent standard deviation less than 5%. This meant that our experimentation methods were precise.

3.2 Testing Results

The following section includes our results for each of the objectives stated in our methodology. The findings in this section are supported with secondary research and engineering experience gained through four years of education at Worcester Polytechnic Institute. These results heavily influenced the conclusions that we made in the following section.

3.2.1 Experimental Procedure

In order to accurately identify mechanical properties of a 3D printed beam, we needed to establish an accurate, reliable, and repeatable experiment. We decided that

a beam deflection experiment to determine an unknown Young's Modulus would be the most appropriate method of quantifying mechanical properties of a 3D printed beam. We then developed a procedure using common mechanical engineering practices. This was designed using the WPI 3901 "Beam Deflection Experiment" procedure as a template. Our goal for this experiment was to measure the deflections caused by the applied loads. Since deflection and applied load are directly proportional, we expected the deflections and loads to have a linear relationship, giving us a constant Young's Modulus output.

The procedure we determined is as follows:

1) First, set up the testing apparatus. Complete this by aligning the front of the testing apparatus flush with the testing table and use a Quik-Grip clamp, or any other viable clamping system to secure the apparatus to the table.

2) Adjust the measuring arm by loosening the horizontal machine screw using a 5/16" allen wrench. Adjust by sliding the arm left and right depending on the length of the specimen that is being tested. Once the desired arm position is obtained, tighten the horizontal machine screw using a 5/16" allen wrench.

3) Slide the specimen into the testing slot on the apparatus. The back of the specimen should touch the vertical machine screw in the middle of the specimen clamp on the apparatus. The front of the specimen should be in line with the vertical ruler without touching. If this is not the case, repeat step 2 until the ruler and the end of the specimen are lined up.

4) Using a 5/16" allen wrench, tighten the middle machine screw on the apparatus clamp until it is flush with the top of the specimen. Next, turn the screw on the rear machine screw on the specimen clamp until the rear of the clamp is the same height of the specimen. This will ensure that the specimen is clamped properly and will sit perfectly horizontal in the apparatus.

5) Next, tie a loop around each of the masses (100g, 200g, 300g, 500g). For this, we recommend using fishing line tested for at least 10-lbs. At the other end of the fishing line, a loop must be tied of approximately 4 cm in diameter. this will be attached to the end of the specimen.

6) Attach the loop of the 100g mass to the end of the specimen. The loop should go on the notch located roughly 1 cm from the end of the specimen. The closer the notch is to the end of the specimen, the more accurately deflection will be measured.

7) Hold the mass so that it is not suspended at the end of the specimen and has no influence on deflection. Read the initial value on the ruler perfectly parallel to the top of the specimen and record this value. Slowly and with control, lower and release the mass so it is suspended at the end of the specimen. Obtain a new ruler measurement by recording the value of the ruler perfectly parallel to the top of the specimen. Subtract the initial and experimental recordings on the ruler and record this as the deflection.

8) Repeat steps 6 and 7 for masses of 200g, 300g, and 500g. Plot recorded values

on an excel sheet and find the mean and standard deviation.

9) Repeat steps 2 through 8 in this procedure using specimens of varying print orientations, 0 to 90 degrees, with 10 degree increments until 10 specimen recordings are obtained.

10) Plot the means and standard deviations of the recordings, repeat using new specimens until results aptly represent the specimens being tested.

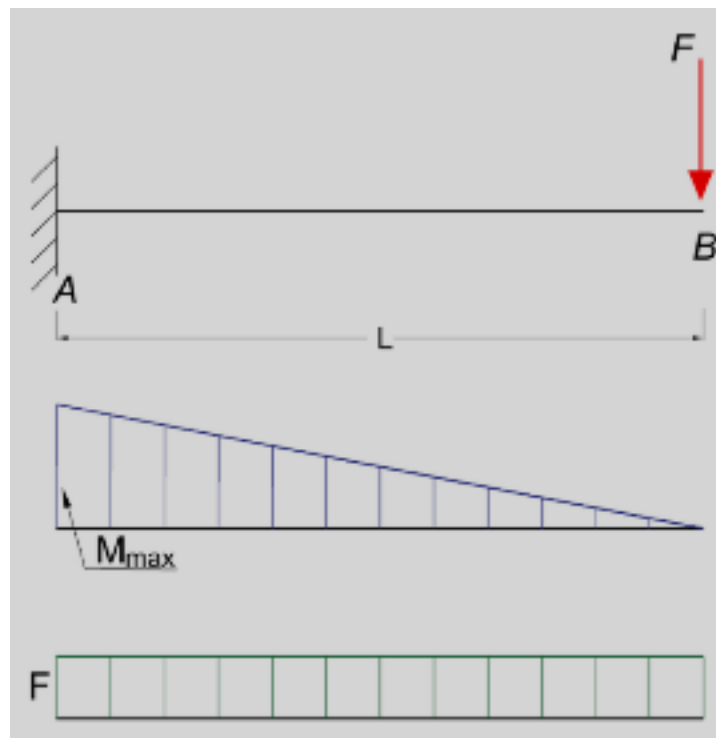*Figure 10. Testing Apparatus Prepared for Experimentation.*

Figure 11. Diagram of a Cantilever Beam under point load and its corresponding bending moment and shear force diagrams.

3.2.2 Experimental Components

The experimental components we chose were selected using multiple means of secondary research and primary research, as well as personal experiences in the field of mechanical engineering experimentation. Our first component, the apparatus, was first designed using CAD software. The apparatus required a sturdy base to be attached to a testing table. The apparatus also required a platform for the specimen to rest perfectly horizontal. Another requirement of the system was that it had a measuring arm that was adjustable and would hold a metric ruler perfectly vertical to allow for accurate measuring. Lastly, it was required for the specimen to be clamped evenly. The end product for the apparatus is shown below.
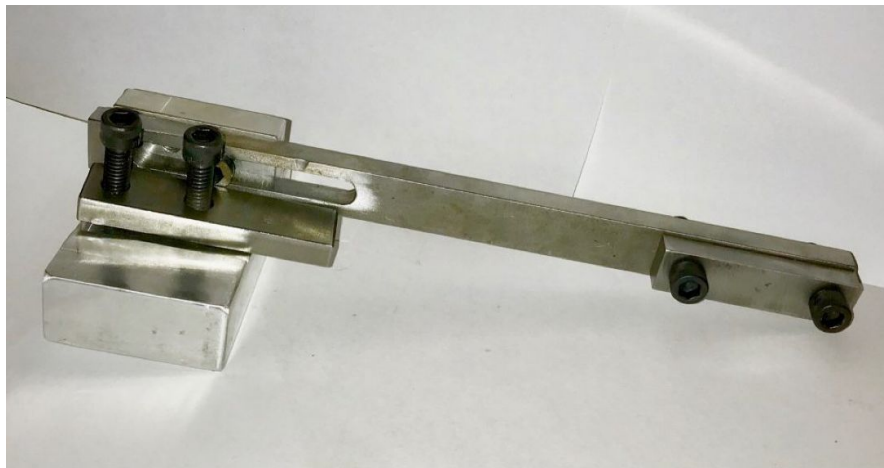
Figure 12. Testing Apparatus.

The apparatus base measures 10cm x 7cm. It was made out of A-2 Steel and uses 5/16" machine screws. The extension arm measures 20 cm long and can be adjusted to measure as short as 10 cm specimens. The specimen clamp can be adjusted by turning the screw in the back to balance the clamping on differing thickness specimens. We chose to use a Quick-Grip clamp to clamp the right side of the apparatus to the testing table because it is a reliable clamp and convenient to use.

The next component we selected was the testing environment. For this, we chose WPI's Foisie Makerspace Lab. This was a controlled area with level testing tables that were readily available for student use. We ensured that we followed the set-up component of the procedure to ensure repetition. After this, we chose our load

determination. For PLA, we decided to use a mass set that was provided by WPI and had been recently calibrated. The range of masses used were 100g-500g. This provided adequate deflections that were distinguishable, but did not bend the PLA specimens past their elastic deformation point. We used the same mass set throughout the testing to ensure consistency. We also chose 10-lb test fishing line to tie the masses to the end of our specimen. We did this because the mass of the string would be insignificant to our testing results and would be strong enough to support up to 500g loads.

Lastly, the most important experimental component we had to determine was the print variable we wanted to isolate and test. We decided that the one independent variable we would have in this beam deflection experiment was the print orientation of the specimens. Through secondary research, or lack thereof, we found that print orientation was a widely under researched variable in 3D printing and we wanted to determine if this variable had a significant impact on the Young's Modulus of the beams. We decided that we would test the print orientation of the specimens on the x-y plane. Each specimen will be printed at 10 degree increments to provide a broad range of values of Young's Modulus over the set.

Figure 13. Mass Set Used in the Experimentation

Figure 14. PLA Specimens used in Testing.

3.2.3 Calibration Results

To calibrate our system, we used an AMS 5598 alloy with a known Elastic Modulus of 193 GPa. The specimens we used were 0.0254m wide, 0.15m long, and had a thickness of 0.9398 mm. The dimensions were constant through all specimens to ensure constant experimental factors. We measured 5 specimens using the procedure stated in section 4.1. Our recorded Young's Modulus of the alloys were 194 GPa with a standard deviation of 2.29%. In engineering experimentation, this is a value that would be widely accepted as a range that can be used for a scientific finding. This value is also only 1 GPa away from the known modulus for AMS 5598, solidifying that our testing procedure is accurate. This 0.5% error can be assumed to be due to minor experimental errors in testing or specimen deformations. Satisfied with our calibration, we then were able to test the PLA specimens with confidence in our findings.

Physical Properties

Grade	Density (kg/m^3)	Elastic Modulus (GPa)	Mean Coefficient of Thermal Expansion (mm/m/°C)			Thermal Conductivity (W/m.K)		Specific Heat 0-100°C (J/kg.K)	Electrical Resistivity (nW.m)
			0-100°C	0-315°C	0-538°C	at 100°C	at 500°C		
304/L/H	8000	193	17.2	17.8	18.4	16.2	21.5	500	720

Figure 15. Physical Properties of AMS 5598.

Material	Mean Experimental Young's Modulus	Standard Deviation	Known Young's Modulus	Percent Error in Experiment
AMS 5598 (Steel)	194 GPa	2.29%	193 GPa	0.518%

Figure 16. Table of Calibration Experiment

3.2.4 Experimentation of PLA Results

The specimens of PLA that we decided to test were modeled using CAD software and sent to the Foisie Innovation Studio FDM 3D Printers. The infill rate of the specimens were held constant at 30%. A 30% infill rate was enough to allow for a strong specimen, but not too much to cause repeated printing failure of our specimens. The prints were printed at 10 degree of orientation increments, starting at 0 degrees and ending at 90 degrees. Figure X. Shows the orientations on a x-y plane. The specimens that were tested were 2.50cm wide, 14 cm long, and had a thickness of 0.417 cm. The dimensions were held constant throughout the testing.

Following the procedure that was laid out in 4.1, we conducted our experiments on four sets of specimens, each set containing one specimen at each 10 degree orientation increment. At 0 degrees, the mean Young's Modulus was 2.109 GPa with a standard deviation of 1.84%. At 10 degrees, the mean Young's Modulus was 2.111 GPa with a standard deviation of 1.38%. At 20 degrees, the mean Young's Modulus was 2.115 GPa, with a standard deviation of 1.60%. At 30 degrees, the mean Young's Modulus was 2.135 GPa, with a standard deviation of 1.97%. At 40 degrees, the Young's Modulus was 2.144 GPa, with a standard deviation of 2.52%. At 50 degrees, the mean Young's Modulus was 2.137 GPa, with a standard deviation of 1.07%. At 60 degrees, the mean Young's Modulus was 2.115 GPa, with a standard deviation of 0.95%. At 70 degrees, the mean Young's Modulus was 2.087 GPa, with a standard deviation of 2.11%. At 80 degrees, the mean Young's Modulus was 2.086 GPa, with a standard deviation of 1.61%. At 90 degrees, the mean Young's Modulus was 2.051 GPa with a standard deviation of 0.90%. A table with this data is provided in the appendix. From this, we were able to determine trends in Young's Modulus according to print

orientation. By following trendlines provided in Figure X, we can infer that 45 degrees had the highest value in Young's Modulus. Another inference that we can make is that 90 degrees had the lowest Young's Modulus to the right side of the peak, 2.051 GPa, and 0 degrees had the lowest Young's Modulus to the left of the peak, with a value of 2.109 GPa. Following this trend we see that the under constant variables, print orientation yields the strongest cantilever beam under unidirectional load at 45 degrees.

Print Orientation	Mean (GPa)	Percent Standard Deviation
0 Degrees	2.109	1.84%
10 Degrees	2.111	1.38%
20 Degrees	2.115	1.60%
30 Degrees	2.136	1.97%
40 Degrees	2.144	2.52%
50 Degrees	2.137	1.07%
60 Degrees	2.115	0.95%
70 Degrees	2.087	2.11%
80 Degrees	2.086	1.61%
90 Degrees	2.051	0.90%

Figure 17. Table of Young's Modulus Testing Data.

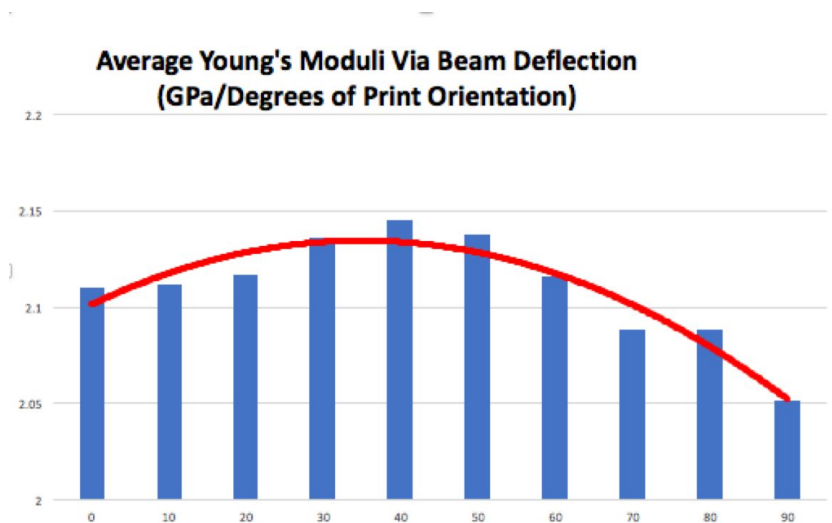*Figure 18: Graph Showing Mean Young's Moduli of Print Orientations.*

4. Numerical Analysis of 3D Printed Model

The next step in our analysis was to have a way to compare the results from the experimental method. This was needed in order to provide evidence to support or disprove any conclusions we may draw from the data gathered in the experimental analysis. Experiments, including those involving 3D printing, are prone to error and unaccounted factors, so we sought a reaffirmation from a purely numerical analytical standpoint that could help provide insight into the results of our experimentation.

4.1 Steps to Perform Numerical Analysis

First, we needed to set key design steps to facilitate the analysis process. We decided on 6 key design steps: 1. Define Procedure, 2. Select FEA software, 3. Design Test Models, 4. Define Material Properties, 5. Test Models, and 6. Assess Reliability of Results

4.1.1 Define Procedure

Next, we needed to define a method to find an experimental Young's Modulus for a 3D printed model in order to compare with the Young's Modulus found using the experimental method. Therefore, after researching the subject and guidance from Professor Hou, we decided to use bending deflection analysis on a CAD model. This method is beneficial because it matches our experimental methodology, which allowed us to not only compare the Young's Modulus of the two methods, but also the beam deflection.

4.1.2 Select FEA software

For this step, we had to decide on which FEA software to use in our analysis. For this, we focused on finding a program that had features relevant to our project, to make the analysis quicker. Another factor taken into account was personal experience with each program, as analysis would be easier on a familiar software.

4.1.3 Design Test Models

The next step was to design the model itself. The problem that arose was that FEA programs are used to analyze solid models with defined material properties, and CAD software creates models based on solid materials, unlike 3D printed models like ours made with less than 100% infill. This meant that a model designed with these programs would not correctly match the experimental models, and would therefore be irrelevant to our experiment. In order to overcome this challenge, we accounted for the layering of the 3D printer by matching the layering pattern and including gaps to simulate the infill. This allowed us to use any CAD software we chose, and more importantly allowed us to model the 3D printed specimen as a solid model.

4.1.4 Define Material Properties

An important component of the methodology was to decide on the material properties of the material to be applied to the CAD model. FEA software requires a fully defined material to be applied to a CAD model before it can begin analysis. This meant that the material had to have an inputted Young's Modulus, which would prevent from finding a numerical value. Additionally, PLA filament is a difficult material to model, because of how it is layered and how comes in various suppliers, each with different material properties. The solution to this problem was to create a custom material that accounted for the unique layering, and using values of the material properties of PLA filament to use as the experimental material.

4.1.5 Test the Models

Based on the previous methodology, we tested the 3D CAD models for a numerical Young's Modulus, which we used to compare with the experimental result to find whether the experimental value had any validity.

4.2 Results of Numerical Analysis of 3D Printed Model

Once the parameters for the analysis were set, the next step was to use the aforementioned procedure to set up and run the numerical analysis of the 3D model.

The results of this testing was used in comparison with the experimental results to influence the conclusions section of this report.

4.2.1 Define Strategy

Based on the previous methodology,we developed the following 5 step procedure:

1) Use a CAD software to create a model to analyze. Adjust the model's design to account for the unique layering of 3D filament, while still being modeled as a solid.

2) Define a custom material, including a placeholder Young's Modulus, to take the place of PLA on the CAD model, using material properties of PLA filament from material datasheets.

3) Create and run a beam deflection analysis on the model, using the same constraints as the experimental procedure (one side rigid, force acting on the other end). Use 500g for the weight to calculate the force acting on the model.

4) After determining the bending deflection that the CAD model undergoes, adjust the Young's Modulus of the custom material up or down based on the comparison with the experimental deflection of specimens.

5) Repeat steps 3 and 4 until the deflection of the CAD model roughly matches that of the experimental specimens. Record the Young's Modulus, and compare it to that of the experimental analysis. .

4.2.2 Select FEA Software

For this analysis, we selected SolidWorks, because the program was well known to all group members, and was available on WPI computers, which made the process

easier. Solidworks contains all kinds of FEA programming, and in our opinion has the best CAD modelling software, so it suites the project well.

4.2.3 Design Test Models

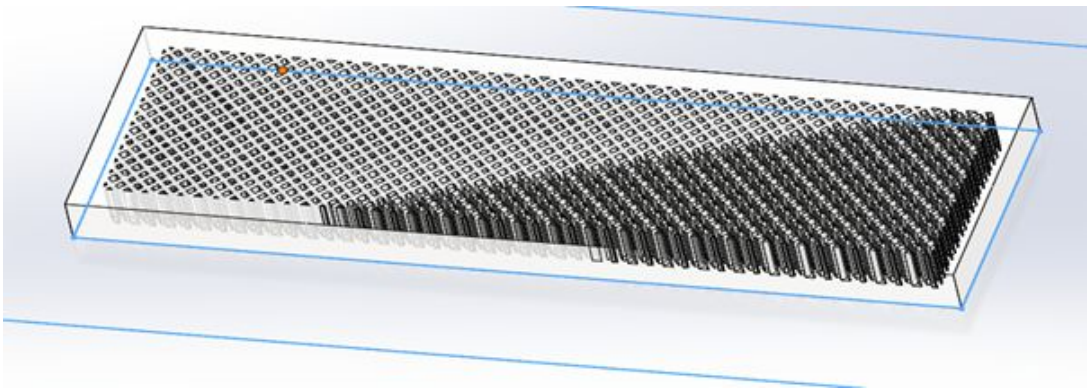The first design for the testing model is shown below:

Figure 19: Original Model with 45-degree orientation

For this experiment we created three models, simulating zero, forty-five, and ninety degrees. Each model was 150mm long, 25mm wide, and 5mm tall, in order to match the test specimens for the experimental section. The sides have a lining that is 5mm thick. In order to create the interior and gaps to simulate 3D filament, we initially used a linear pattern of .5mm thick walls crosshatched on each other for the forty-five degrees. For the zero and ninety degrees, the walls were parallel with the outer walls. These walls were .5mm apart, and extended to all edges of the model. The problem that arose was that there were simply too many data points with all the interior walls. SolidWorks crashed several times, forcing us to adjust the model further. To accomplish this, we multiplied the size of the walls, as well as the gaps between the walls, by three. Therefore, as shown in the figure below, our finished models had interior walls that were 1.5mm thick, with 1.5mm gaps. This allowed us to simplify the model so it could be run while maintaining the same ratio of material to space.
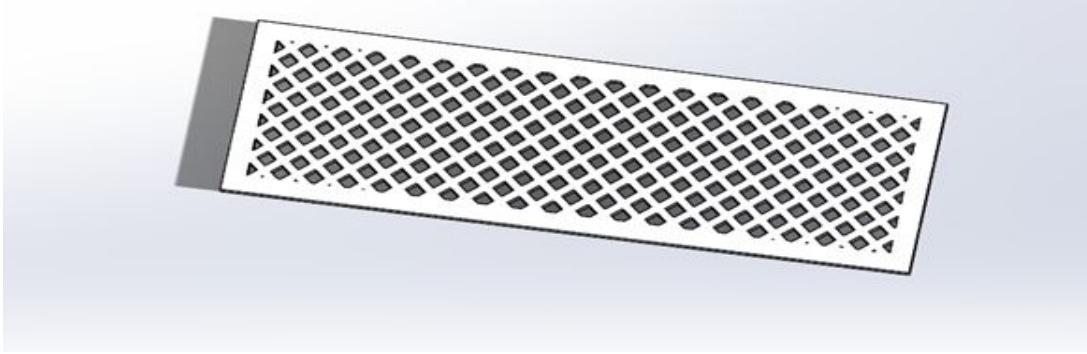
Figure 20: Adjusted model with 45-degree orientation

4.2.4 Define Material Properties

Next we created a custom material. For its properties, we researched various PLA filament suppliers and collected data on the material properties of each. We then found a rough average of these to give the baseline values for PLA as a whole. The material properties are listed below (at 30% infill):

Layer Height	Diameter of Filament	Density	Tensile Strength	Elastic Modulus	Flexural Modulus
.14 mm	2.24 mm	1.26g/cm^3	9.8 MPa	1740 MPa	1225 MPa

Figure 21: Material Properties of Custom Material

4.2.5 Testing the Models

The last step was to set up and run the analysis. For the analysis set up, we secured the right face of the model (the short end) to be completely immovable, to simulate the testing apparatus. Next, a force of 4.91 Newtons was applied to the opposite end to simulate the 500-gram weight. Then the analysis was run, for the 0, 45, and 90-degree orientations, as shown below.
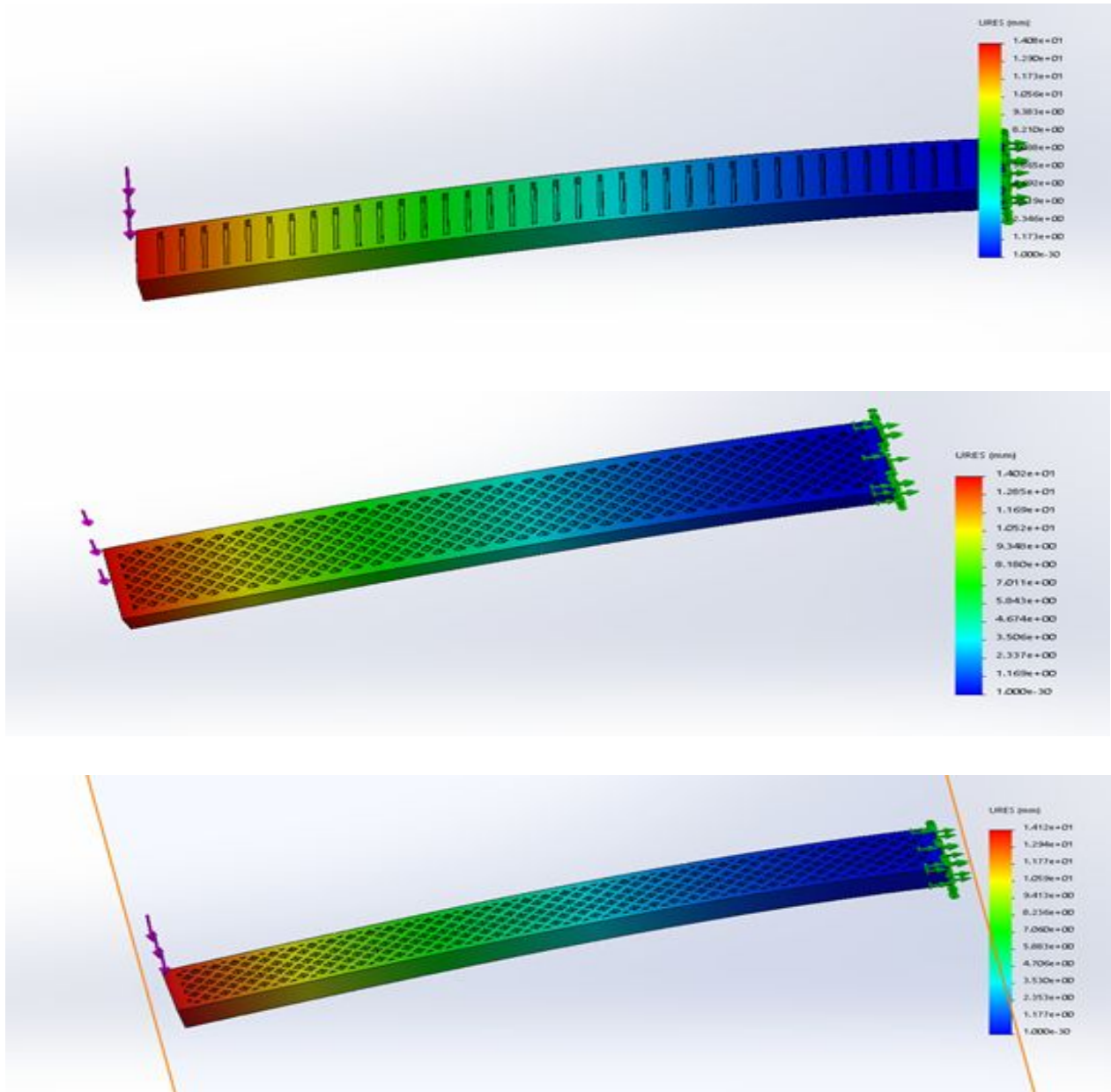
Figure 22: Deflection spectrum of (in order) 0,45, and 90-degree print orientations

Finally, we determined the experimental Young's Modulus of each of the CAD models and compared it with the results from the experimental analysis.

Orientation (degrees)	Experimental Young's Modulus (GPa)	Numerical Young's Modulus (GPa)	Error (%)
0	2.109	2.06	1.37
45	2.14	2.1	1.87
90	2.051	2.02	1.51

Figure 23: Comparison of Numerical and Experimental Result

5. Microstructure Analysis

Polylactic Acid (PLA) is a biodegrading thermoplastic aliphatic polyester commonly used in recreational applications (Rohringer, 2019). When PLA is being processed through the printer, it quickly cools down and solidifies. Thermoplastic chains form the fundamental structure of PLA. These chains are formed by crystal cores based on PLA molecules. The chains are stacked together with the inner cohesion bonding forces and form the boundaries of the basic printing patterns as the user's design. In our case, the basic printing pattern was square. This was a default preset in the FDM printer we used to print our specimens. Each infill geometry is described by the geometric shape which was repeated throughout the interior of the object. These geometric shapes would line up perpendicular to the print axis. Each geometric shape have multiple main axes based on its orientation relative to the geometric shape. As we applied a force on the end of the printed specimen, the force would get distributed along the length of the specimen. The load would then distribute to the bonding boundaries on the polymer chain of the thermoplastic. This explains the performance of the printed bars under each print orientation.
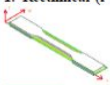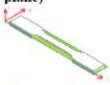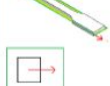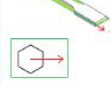
Infill Geometry + Orientation	Fracture Notes			
1. Rectilinear (l-w plane)		6. Rectilinear 45 (l-w plane)	
2. Hexagonal Flat (l-w plane)	Failed near end of gauge length	7. Hexagonal Sharp (l-w plane)	
3. Rectilinear (l-w plane)		8. Shell	Failed near end of gauge length
		9. Solid	
		10. Hexagonal Sharp (l-w plane)	
4. Rectilinear (l-w plane)	Failed near end of gauge length		
		11. Shell	Failed Outside Gauge length
5. Rectilinear 45 (l-t plane)	Failed near end of gauge length	12. Hexagonal Flat (l-w plane)	Failed Outside Gauge length

Figure 24: Examples of possible basic geometries and orientations.

(from Farbman, Daniel & McCoy, Chris. (2016). Materials Testing of 3D Printed ABS and PLA Samples to Guide Mechanical Design.)

6. Conclusion

Through our testing and finite model analysis, we can conclude confidently that print orientation affects the Young's Modulus of 3D printed beams. We conclude that under constant variables, cantilever beams of PLA have a higher Young's Modulus when subjected to unidirectional loads if the print orientation is 45 degrees. In addition, prints oriented at 0 and 90 degrees result in the lowest Young's Modulus.

After completing series of testing and developing a corresponding finite element model, we then assessed the reliability of our findings using our testing experience as support. The first thing that stood out to us was the trend of the graph of the specimens. We found it odd that the strength peaked in the middle and not at either edge. Given that all of our standard deviations

were low and our system was calibrated within 1%, we can trust our findings. We then were able to support these findings following a finite model. The finite model results only had a variance under 1.75% from our experimental values. This discrepancy can be considered due to print quality and recording accuracy. Overall, our findings can be considered accurate as it represents the trends of the data obtained.

As the manufacturing industry seeks to drastically shift their focus to additive manufacturing, our work will serve as a template to maximize Young's Modulus within a 3D printed beam. The applications of our work are multiplicitous. The automotive, aerospace, medical, architectural, and pharmaceutical industries all rely on additive manufacturing. An understanding and predictability of additively manufactured objects is pivotal to their success and future growth.

We recommend that future work be done that would help reinforce our findings. Our recommendations for further projects are as follows:

- Young's Modulus testing for non-PLA materials

- Young's Modulus testing for other geometries

- Young's Modulus testing for other variables such as printing temperature, infill rate, and feed height

- Physical properties testing (other than Young's Modulus)

- Physical properties influenced by different printer types

These recommendations were developed from feedback from peers when presenting our project, as well as recommendations we developed throughout the duration of the project. The more research done on the influences on physical properties, the more successful the field of additive manufacturing will be in the future. Overall, the project was successful in finding a new means to help optimize the mechanical properties associated with 3D printed specimens.

Works Cited

1. Julien Gardan (2016) Additive manufacturing technologies: state of the art and trends, International Journal of Production Research, 54:10, 3118-3132, DOI: 10.1080/00207543.2015.1115909

2. Dizon, J., Espera, A., Chen, Q., & Advincula, R. (2018). Mechanical characterization of 3D-printed polymers. *Additive Manufacturing*, *20*, 44–67. https://doi.org/10.1016/j.addma.2017.12.002

3. Grames, E. (2018, September 29). 3D Printing Layer Height - How Much Does It Matter? Retrieved from https://all3dp.com/2/3d-printer-layer-height-how-much-does-it-matter/

4. Lunt, J. (1998). Large-scale production, properties and commercial applications of polylactic acid polymers. *Polymer Degradation and Stability*, *59*(1), 145–152. https://doi.org/10.1016/S0141-3910(97)00148-1

5. McCue, T. (2018, June 22). Wohlers Report 2018: 3D Printer Industry Tops $7 Billion. Retrieved April 24, 2019, from https://www.forbes.com/sites/tjmccue/2018/06/04/wohlers-report-2018-3d-printer-industry-rises-21-percent-to-over-7-billion/#1d059e712d1a

6. Molitch-Hou, Michael. "FEA Analysis and Predicting the Performance of 3D Printing." *Engineering.com*, 8 Nov. 2016, www.engineering.com/3DPrinting/3DPrintingArticles/ArticleID/13614/FEA-Analysis-and-Predicting-the-Performance-of-3D-Printing.aspx.

7. Most used 3D printing materials worldwide 2018 | Statistic. (2018, July). Retrieved from https://www.statista.com/statistics/800454/worldwide-most-used-3d-printing-materials/

8. Reichental, Avi. "The Future Of 3-D Printing." *Forbes*, Forbes Magazine, 23 Jan. 2018, www.forbes.com/sites/forbestechcouncil/2018/01/23/the-future-of-3-d-printing/#57ed002b65f6.

9. Sawant, R., & Kakade, P. (2018, October). 3D Printing Market by Technology [Stereolithography (SLA), Fused Deposition Modelling (FDM), Selective Laser Sintering (SLS), Electron Beam Melting (EBM), Digital Light Processing (DLP), and Others], Component (Hardware, Software, and Services), and End User (Automotive, Healthcare, Industrial, Consumer Electronics, Aerospace & Defense, and Others): Global Opportunity Analysis and Industry Forecast, 2019 - 2025. Retrieved April 24, 2019, from https://www.alliedmarketresearch.com/3d-printing-market

10. Siber, B. (2018, November 26). Infill (3D Printing) – What It Means and How to Use It. Retrieved from https://all3dp.com/2/infill-3d-printing-what-it-means-and-how-to-use-it/

11. "Technical Data Sheet ." Innofil3D , 7 Oct. 2017.

12. SmarTech Report Show Low-cost 3D Printing Market Is Alive and Healthy. (2018, April 14). Retrieved April 24, 2019, from

https://www.3dprintingmedia.network/new-smartech-report-show-low-cost-3d-printing-market-is-alive-and-healthy/

13. What is ABS Material? (n.d.). Retrieved from
https://www.plasticextrusiontech.net/resources/what-is-abs-material/

14. 3D Printing Market Size, Share & Analysis | 3DP Industry Report, 2025. (2018, October). Retrieved April 24, 2019, from
https://www.grandviewresearch.com/industry-analysis/3d-printing-industry-analysis

15. 3D Matter. (n.d.). FDM 3D Printing materials compared. Retrieved from
https://www.3dhubs.com/knowledge-base/fdm-3d-printing-materials-compared

16. 3D Printing Trends 2019. (n.d.). Retrieved April 24, 2019, from
https://www.3dhubs.com/get/trends/

17. Selective Laser Sintering, Birth of an Industry,
http://www.me.utexas.edu/news/news/selective-laser-sintering-birth-of-an-industry

18. EBM® Electron Beam Melting
http://www.arcam.com/technology/electron-beam-melting/

19. Introduction to Material Jetting
https://www.3dhubs.com/knowledge-base/introduction-material-jetting-3d-printing

19. Manoj. "STAAD PRO AND SPREADSHEETS."

   STAAD PRO AND SPREADSHEETS, 1 Jan. 1970,

   www.bentleystaadpro.blogspot.com

20. "Finite Element Analysis (FEA)." *Thirteen Design\ Irish Engineering & Graphic*

Design Consultancy, www.thirteendesignconsultancy.com/finite-element-analysis-fea

Appendix

The following appendix includes key equations used in experimentation as well as relevant data collected.

The formula for Young's Modulus for this would be as follows:

$$E = FL^3/3\delta I$$

Where:

E = modulus of elasticity

F = force applied at B

L = Length of Beam (to B)

δ = maximum deflection in B

I = moment of Inertia

Appendix 1. Formulas and Expressions used to Calculate Young's Modulus

Subject	Thickness (m)	Width (m)	Length (m)	Deflection @ 100 g	Deflection @ 200 g	Deflection @500g	Moment of Inertia	Young's Modulus @ 100 g	Young's Modulus @ 200 g	Young's Modulus @ 500 g	Mean Young's Modulus
AMS 5598	0.0009398	0.0254	0.15	3.20E-03	0.0065	0.0156	1.75695E-12	1.96E+11	1.93277E+11	2.0133E+11	1.97E+11
AMS 5598	0.0009398	0.0254	0.15	0.0033	0.0065	0.0158	1.75695E-12	1.90348E+11	1.93277E+11	1.98781E+11	1.94E+11
AMS 5598	0.0009398	0.0254	0.15	0.0032	0.0065	0.016	1.75695E-12	1.96297E+11	1.93277E+11	1.96297E+11	1.95E+11
AMS 5598	0.0009398	0.0254	0.15	0.0033	0.0065	0.0157	1.75695E-12	1.90348E+11	1.93277E+11	2.00047E+11	1.95E+11
AMS 5598	0.0009398	0.0254	0.15	0.0034	0.0066	0.0158	1.75695E-12	1.8475E+11	1.90348E+11	1.98781E+11	1.91E+11
Mean:	1.94 GPa	Std. Dev.:	2.29%								

Appendix 2. Table of Results to Calibration of Apparatus

Specimen	Thickness (m)	Width (m)	Length (m)	Deflection 100g	Deflection 200 g	Deflection 500 g	MOI
0 degrees #1	0.0041656	0.025019	0.14	0.0027	0.0056	0.0142	1.507E-10
10 degrees #1	0.0041656	0.025019	0.14	0.0028	0.0056	0.0141	1.50703E-10
20 degrees #1	0.0041656	0.025019	0.14	0.0028	0.0054	0.0142	1.50703E-10
30 degrees #1	0.0041656	0.025019	0.14	0.0028	0.0054	0.0141	1.50703E-10
40 degrees #1	0.0041656	0.025019	0.14	0.0028	0.0054	0.0142	1.50703E-10
50 degrees #1	0.0041656	0.025019	0.14	0.0028	0.0056	0.0141	1.50703E-10
60 degrees #1	0.0041656	0.025019	0.14	0.0028	0.0056	0.0143	1.50703E-10
70 degrees #1	0.0041656	0.025019	0.14	0.0029	0.0058	0.0143	1.50703E-10
80 degrees #1	0.0041656	0.025019	0.14	0.0029	0.0058	0.0144	1.50703E-10
90 degrees #1	0.0041656	0.025019	0.14	0.003	0.0058	0.0146	1.507E-10
0 degrees #2	0.0041656	0.025019	0.14	0.0029	0.0056	0.0143	1.507E-10
10 degrees #2	0.0041656	0.025019	0.14	0.0029	0.0055	0.0144	1.50703E-10
20 degrees #2	0.0041656	0.025019	0.14	0.0029	0.0057	0.0144	1.50703E-10
30 degrees #2	0.0041656	0.025019	0.14	0.0028	0.0056	0.0143	1.50703E-10
40 degrees #2	0.0041656	0.025019	0.14	0.0027	0.0056	0.0141	1.50703E-10
50 degrees #2	0.0041656	0.025019	0.14	0.0028	0.0055	0.014	1.50703E-10
60 degrees #2	0.0041656	0.025019	0.14	0.0028	0.0056	0.0141	1.50703E-10
70 degrees #2	0.0041656	0.025019	0.14	0.0029	0.0055	0.0143	1.50703E-10
80 degrees #2	0.0041656	0.025019	0.14	0.0028	0.0055	0.0145	1.50703E-10
90 degrees #2	0.0041656	0.025019	0.14	0.0029	0.0058	0.0145	1.507E-10
0 degrees #3	0.0041656	0.025019	0.14	0.0028	0.0057	0.0143	1.507E-10
10 degrees #3	0.0041656	0.025019	0.14	0.0028	0.0056	0.0142	1.50703E-10
20 degrees #3	0.0041656	0.025019	0.14	0.0028	0.0055	0.0141	1.50703E-10
30 degrees #3	0.0041656	0.025019	0.14	0.0027	0.0056	0.0141	1.50703E-10
40 degrees #3	0.0041656	0.025019	0.14	0.0027	0.0056	0.0142	1.50703E-10
50 degrees #3	0.0041656	0.025019	0.14	0.0028	0.0055	0.0141	1.50703E-10
60 degrees #3	0.0041656	0.025019	0.14	0.0028	0.0056	0.0143	1.50703E-10
70 degrees #3	0.0041656	0.025019	0.14	0.0029	0.0055	0.0143	1.50703E-10
80 degrees #3	0.0041656	0.025019	0.14	0.0028	0.0057	0.0145	1.50703E-10
90 degrees #3	0.0041656	0.025019	0.14	0.0029	0.0057	0.0143	1.507E-10

Appendix 3. Deflection Data for Young's Modulus Experiment on 3 sets of specimens.

Specimen	Youngs Modulus 100	Youngs Modulus 200	Youngs Modulus 500	Average	Percent Standard Deviation
0 degrees #1	2205193484	2126436573	2096486763	2142705607	2.620508831
10 degrees #1	2126436573	2126436573	2111355463	2121409537	0.41043858
20 degrees #1	2126436573	2205193484	2096486763	2142705607	2.620508831
30 degrees #1	2126436573	2205193484	2111355463	2147661840	2.346330468
40 degrees #1	2126436573	2205193484	2096486763	2142705607	2.620508831
50 degrees #1	2126436573	2126436573	2111355463	2121409537	0.41043858
60 degrees #1	2126436573	2126436573	2081826016	2111566388	1.21975409
70 degrees #1	2053111174	2053111174	2081826016	2062682788	0.803735874
80 degrees #1	2053111174	2053111174	2067368891	2057863747	0.400011734
90 degrees #1	1984674135	2053111174	2039048769	2025611360	1.784310113
0 degrees #2	2053111174	2126436573	2081826016	2087124588	1.770318085
10 degrees #2	2053111174	2165099057	2067368891	2095193041	2.909453426
20 degrees #2	2053111174	2089130669	2067368891	2069870245	0.876362091
30 degrees #2	2126436573	2126436573	2081826016	2111566388	1.21975409
40 degrees #2	2205193484	2126436573	2111355463	2147661840	2.346330468
50 degrees #2	2126436573	2165099057	2126436573	2139324068	1.043404101
60 degrees #2	2126436573	2126436573	2111355463	2121409537	0.41043858
70 degrees #2	2053111174	2165099057	2081826016	2100012082	2.769829463
80 degrees #2	2126436573	2165099057	2053111174	2114882268	2.689558598
90 degrees #2	2053111174	2053111174	2053111174	2053111174	1.64226E-14
0 degrees #3	2126436573	2089130669	2081826016	2099131086	1.139882842
10 degrees #3	2126436573	2126436573	2096486763	2116453303	0.817005098
20 degrees #3	2126436573	2165099057	2111355463	2134297031	1.298818007
30 degrees #3	2205193484	2126436573	2111355463	2147661840	2.346330468
40 degrees #3	2205193484	2126436573	2096486763	2142705607	2.620508831
50 degrees #3	2126436573	2165099057	2111355463	2134297031	1.298818007
60 degrees #3	2126436573	2126436573	2081826016	2111566388	1.21975409
70 degrees #3	2053111174	2165099057	2081826016	2100012082	2.769829463
80 degrees #3	2126436573	2089130669	2053111174	2089559472	1.754655979
90 degrees #3	2053111174	2089130669	2081826016	2074689286	0.917764584
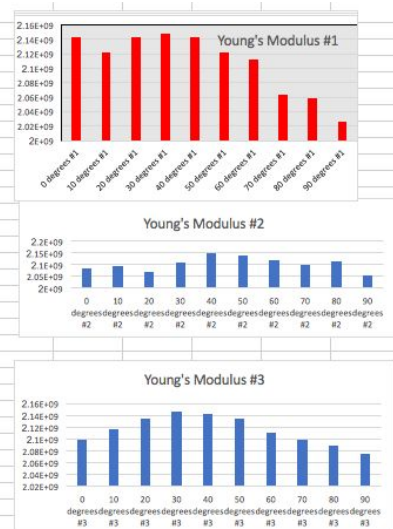
Appendix 4. Young's Moduli and Corresponding Graphs for 3 Specimens